

On Solving Three-dimensional Laplacian Problems in a Multiply Connected Domain Using the Multiple Scale Trefftz Method

Cheng-Yu Ku^{1,2}

Abstract: This paper proposes the numerical solution of three-dimensional Laplacian problems in a multiply connected domain using the collocation Trefftz method with multiple source points. A numerical solution for three-dimensional Laplacian problems was approximated by superpositioning T-complete functions formulated from 36 independent functions satisfying the governing equation in the cylindrical coordinate system. To deal with complicated problems for multiply connected domain, we adopted the generalized multiple source point boundary collocation Trefftz method which allows many source points in the Trefftz formulation without using the decomposition of the problem domain. In addition, to mitigate a severely ill-conditioned system of linear equations, this study adopted the newly developed multiple scale Trefftz method and the dynamical Jacobian-inverse free method. Numerical solutions were conducted for five three-dimensional groundwater flow problems in a simply connected domain, an infinite domain, a doubly connected domain, and a multiply connected domain. The results revealed that the proposed method can obtain accurate numerical solutions for three-dimensional Laplacian problems in a multiply connected domain, yielding a superior convergence in numerical stability to that of the conventional Trefftz method.

Keywords: Trefftz method, Ill-conditioned, Multiply connected domain, The multiple scale, Three-dimensional.

1 Introduction

The Trefftz method [Trefftz (1926)] is a meshless numerical method for solving boundary value problems where approximate solutions are expressed as a linear combination of functions automatically satisfy governing equations. According

¹ Department of Harbor and River Engineering, National Taiwan Ocean University, Keelung, Taiwan.

² Corresponding author. Email: chkst26@mail.ntou.edu.tw

to Kita and Kamiya (1995), Trefftz methods are classified as either direct or indirect formulations. Unknown coefficients are determined by matching boundary conditions. Li et al. (2008) provided a comprehensive comparison of the Trefftz method collocation and other boundary methods concluding that the collocation Trefftz method (CTM) is the simplest algorithm and provides the most accurate solutions with optimal numerical stability. To deal with complicated problems for the multiply connected domain with genus greater than one in the Trefftz method, one needs to use the domain decomposition method [Kita, Kamiya, and Iio (1999)] which decomposes the problem domain into several simply connected subdomains and to use the Trefftz method in each one. The domain decomposition method may successfully resolve the difficulty when facing the multiply connected domain with genus greater than one. However, the artificial boundaries introduced in the domain decomposition method are not unique and depend on the users' preference.

The Trefftz method has been increasingly used because it is a numerical method applicable for easily and rapidly solving boundary value problems. Kita et al. (2005) described the application of the Trefftz method for solving a three-dimensional Poisson equation; an inhomogeneous term containing the unknown function was approximated using a polynomial function in the Cartesian coordinates to determine the solution for the Poisson equation. Applications of the Trefftz method in engineering problems, such as Laplace and biharmonic equations [Chen et al. (2007)] and the two-dimensional boundary detection problem [Fan et al. (2012)], have been reported. Because of complexity, most applications of the Trefftz method are still based on two-dimensional problems.

This study presents a numerical solution for three-dimensional Laplacian problems in a multiply connected domain by using the CTM with multiple source points based on a cylindrical coordinate system. In the present formulation, the unknown solution is approximated by superpositioning the T-complete functions satisfying the governing equation in the cylindrical coordinate system. The T-complete functions are composed of a set of linearly independent vectors. The basis for the T-complete functions includes 36 linearly independent functions. The generalized multiple source point boundary collocation Trefftz method [Yeih et al. (2010); Dong and Atluri (2012)] is adopted to deal with the problems in a multiply connected domain. For the indirect Trefftz formulation, the solution is expressed as the linear combination of these basic functions. Because using conventional CTMs results in extremely ill-conditioned linear equation systems, particularly when solving three-dimensional Laplacian problems, the resulting numerical solutions may be unstable. In order to obtain an accurate solution of the linear equations, special techniques [Chen, Cho, and Golberg (2006); Liu (2007)], e.g., the Tikhonov regularization, the singular value decomposition conditioning by a suitable precon-

ditioner, and truncated singular value decomposition, may be required. Liu (2007) has modified the Trefftz method, and refined it by incorporating a single characteristic length into the T-complete functions to reduce substantially the condition number of the resulting linear equation system. Moreover Liu (2008) proposed the multiple scale Trefftz method for solving the inverse Cauchy problem for the Laplace equation. Because applying the multiple-scale concept can significantly reduce condition numbers, the numerical solution for three-dimensional Laplacian problems was approximated based on the multiplescale Trefftz method in this study. In addition to the multiple scale Trefftz method, we adopted the general dynamical method proposed by Ku et al. (2011). The general dynamical method is based on the scalar homotopy method and demonstrates great numerical stability for solving linear algebraic equations particularly for systems involving ill-conditioned problems. With the combination of the multiple scale Trefftz method and the dynamical Jacobian-inverse free method (DJIFM), solutions for extremely ill-conditioned systems of linear equations for three-dimensional Laplacian problems can be obtained. The remainder of this paper is organized as follows: Section 2 describes the formulation of the Trefftz method for three-dimensional Laplacian problems in a multiply connected domain based on cylindrical coordinate systems. Section 3.1 explains the derivation of the multiplescale Trefftz method for solving three-dimensional Laplacian problems, and Section 3.2 demonstrates the incorporation of the DJIFM for solving the extremely ill-conditioned system of linear equations for three-dimensional Laplacian problems. In Section 4, the numerical solutions for four problems involving three-dimensional groundwater flow problems are addressed. Finally, conclusions are drawn in Section 5.

2 Trefftz formulation based on the cylindrical coordinate system

Considering a three-dimensional domain Ω enclosed by a boundary Γ , the Laplace governing equation is expressed as

$$\nabla^2 u = 0 \quad \text{in } \Omega \quad (1)$$

and

$$u = f \quad \text{on } \Gamma_D \quad (2)$$

$$u_n = \frac{\partial u}{\partial n} = \bar{q} \quad \text{on } \Gamma_N \quad (3)$$

where Ω denotes the object domain under consideration, n denotes the outward normal direction, Γ_D denotes the boundary where the Dirichlet boundary condition is given, and Γ_N denotes the boundary where the Neumann boundary condition is

given. In this study, we adopted the cylindrical coordinate system, as shown in Fig. 1. The Laplace governing equation in the cylindrical coordinate system can be written as

$$\frac{\partial^2 u}{\partial \rho^2} + \frac{1}{\rho} \frac{\partial u}{\partial \rho} + \frac{1}{\rho^2} \frac{\partial^2 u}{\partial \theta^2} + \frac{\partial^2 u}{\partial z^2} = 0. \tag{4}$$

In the Trefftz method, the unknown solution is approximated by superpositioning the T-complete functions satisfying the governing equation, as shown in Eq. (4). The T-complete functions are composed of a set of linearly independent functions.

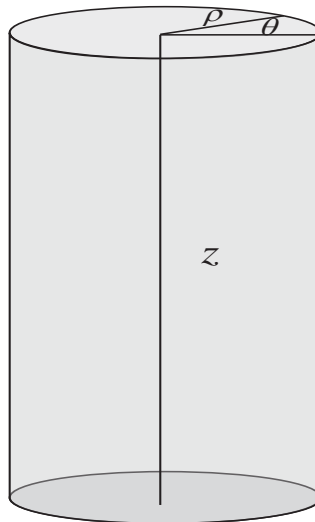


Figure 1: The cylindrical coordinate system.

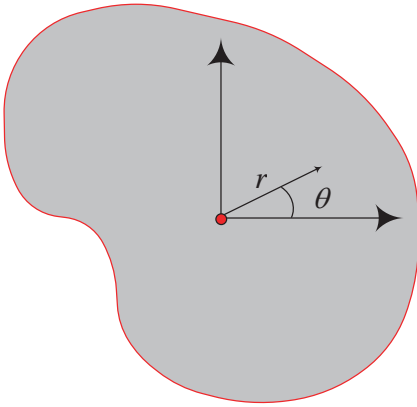
For a simply connected domain illustrated in Fig. 2(a), one may locate a source point inside the domain and the T-complete basis functions are expressed

$$\mathbf{N} = \{\overline{N}_1, \overline{N}_2, \overline{N}_3, \dots, \overline{N}_{18}\}. \tag{5}$$

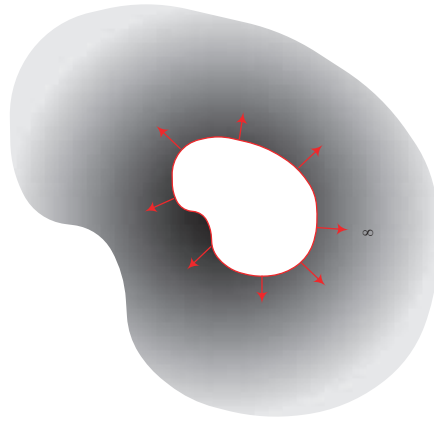
For an infinite domain with a cavity as illustrated in Fig. 2(b), one may locate a source point inside the cavity and the T-complete basis functions are expressed

$$\mathbf{N} = \{\overline{N}_1, \overline{N}_{19}, \overline{N}_{23}, \overline{N}_{24}, \overline{N}_{29}, \overline{N}_{30}, \overline{N}_{31}, \overline{N}_{32}, \overline{N}_{33}, \overline{N}_{34}\}. \tag{6}$$

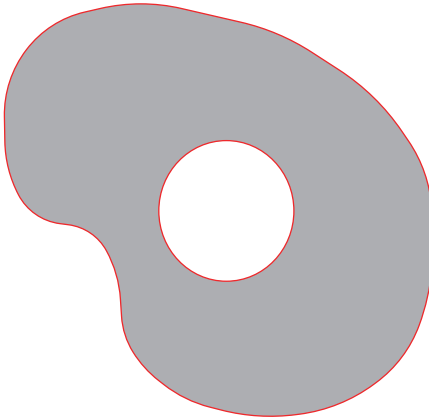
For the doubly and multiply connected domains with genus greater than one, as illustrated in Fig. 2(c) and (d), the domain decomposition method was often used.



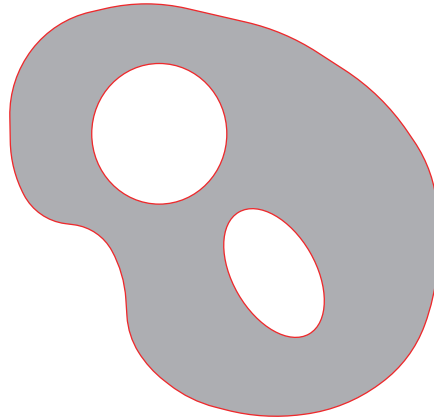
(a) a simply connected domain



(b) an infinite domain with a cavity



(c) a doubly connected domain



(d) a multiply connected domain

Figure 2: Illustration of four different types of domain.

For the domain decomposition method, extra works are needed to decompose the problem domain into several simply connected subdomains. On the real boundary, the Trefftz method requires the approximate solution to satisfy the boundary conditions at each collocation point. On the other hand, the continuity conditions are required to adopt to connect the adjacent subdomains on artificial boundaries. In present formulation, we adopted the generalized multiple source point boundary collocation Trefftz method. Instead of decomposing the problem domain into several simply connected subdomains, one can locate many source points in the domain. Usually, at least one source point inside the cavity is required. Because

no extra collocation points on the artificial boundaries are required, the proposed method may be more efficient, particularly in three-dimensional problems. The T-complete basis functions for the doubly and multiply connected domains with genus greater than one, can be expressed

$$\mathbf{N} = \{\overline{N_1}, \overline{N_2}, \overline{N_3}, \dots, \overline{N_{36}}\}. \tag{7}$$

Using this formulation, we can deal with a multiply connected domain with genus greater than one without introducing artificial boundaries. The basis \mathbf{N} for the above T-complete functions includes 36 functions obtained from the separation of variables in the cylindrical coordinate system, which are listed in Table 1.

Table 1: The basis for the T-complete functions.

$\overline{N_1}$	1	$\overline{N_2}$	z
$\overline{N_3}$	$\cosh(kz)J_0(k\rho)$	$\overline{N_4}$	$\sinh(kz)J_0(k\rho)$
$\overline{N_5}$	$\cos(kz)I_0(k\rho)$	$\overline{N_6}$	$\sin(kz)I_0(k\rho)$
$\overline{N_7}$	$\cos(\nu\theta)\cosh(kz)J_\nu(k\rho)$	$\overline{N_8}$	$\sin(\nu\theta)\sinh(kz)J_\nu(k\rho)$
$\overline{N_9}$	$\cos(\nu\theta)\sinh(kz)J_\nu(k\rho)$	$\overline{N_{10}}$	$\sin(\nu\theta)\cosh(kz)J_\nu(k\rho)$
$\overline{N_{11}}$	$\cos(\nu\theta)\cos(kz)I_\nu(k\rho)$	$\overline{N_{12}}$	$\sin(\nu\theta)\sin(kz)I_\nu(k\rho)$
$\overline{N_{13}}$	$\cos(\nu\theta)\sin(kz)I_\nu(k\rho)$	$\overline{N_{14}}$	$\sin(\nu\theta)\cos(kz)I_\nu(k\rho)$
$\overline{N_{15}}$	$\rho^\nu \cos(\nu\theta)$	$\overline{N_{16}}$	$\rho^\nu \sin(\nu\theta)$
$\overline{N_{17}}$	$z\rho^\nu \cos(\nu\theta)$	$\overline{N_{18}}$	$z\rho^\nu \sin(\nu\theta)$
$\overline{N_{19}}$	$\ln \rho$	$\overline{N_{20}}$	$z \ln \rho$
$\overline{N_{21}}$	$\cosh(kz)Y_0(k\rho)$	$\overline{N_{22}}$	$\sinh(kz)Y_0(k\rho)$
$\overline{N_{23}}$	$\cos(kz)K_0(k\rho)$	$\overline{N_{24}}$	$\sin(kz)K_0(k\rho)$
$\overline{N_{25}}$	$\cos(\nu\theta)\cosh(kz)Y_\nu(k\rho)$	$\overline{N_{26}}$	$\sin(\nu\theta)\sinh(kz)Y_\nu(k\rho)$
$\overline{N_{27}}$	$\cos(\nu\theta)\sinh(kz)Y_\nu(k\rho)$	$\overline{N_{28}}$	$\sin(\nu\theta)\cosh(kz)Y_\nu(k\rho)$
$\overline{N_{29}}$	$\cos(\nu\theta)\cos(kz)K_\nu(k\rho)$	$\overline{N_{30}}$	$\sin(\nu\theta)\sin(kz)K_\nu(k\rho)$
$\overline{N_{31}}$	$\cos(\nu\theta)\sin(kz)K_\nu(k\rho)$	$\overline{N_{32}}$	$\sin(\nu\theta)\cos(kz)K_\nu(k\rho)$
$\overline{N_{33}}$	$\rho^{-\nu} \cos(\nu\theta)$	$\overline{N_{34}}$	$\rho^{-\nu} \sin(\nu\theta)$
$\overline{N_{35}}$	$z\rho^{-\nu} \cos(\nu\theta)$	$\overline{N_{36}}$	$z\rho^{-\nu} \sin(\nu\theta)$

In the above table, I_0 and I_ν are the modified Bessel functions of the first kind of zero order and of ν order, respectively. J_0 and J_ν are the Bessel functions of the first kind of zero order and of ν order, respectively. K_0 and K_ν are the modified Bessel functions of the second kind of zero order and of ν order, respectively. Y_0 and Y_ν are the Bessel functions of the second kind of zero order and of ν order, respectively.

For the indirect Trefftz formulation one can say that the solutions for a simply connected domain, an infinite domain with a cavity, and the doubly and multiply

connected domains are written as the linear combination of these basis functions as shown in Eqs. (8), (9), and (10), respectively.

$$\begin{aligned}
 U = & a + bz + \sum_{k=1}^g \left\{ c_{1k} \cosh(kz)J_0(k\rho) + c_{2k} \sinh(kz)J_0(k\rho) \right. \\
 & \left. + c_{3k} \cos(kz)I_0(k\rho) + c_{4k} \sin(kz)I_0(k\rho) \right. \\
 & \left. + \sum_{v=1}^h \left\{ \begin{aligned} & d_{1kv} \cos(v\theta) \cosh(kz)J_v(k\rho) + d_{2kv} \sin(v\theta) \sinh(kz)J_v(k\rho) \\ & + d_{3kv} \cos(v\theta) \sinh(kz)J_v(k\rho) + d_{4kv} \sin(v\theta) \cosh(kz)J_v(k\rho) \\ & + d_{5kv} \cos(v\theta) \cos(kz)I_v(k\rho) + d_{6kv} \sin(v\theta) \sin(kz)I_v(k\rho) \\ & + d_{7kv} \cos(v\theta) \sin(kz)I_v(k\rho) + d_{8kv} \sin(v\theta) \cos(kz)I_v(k\rho) \end{aligned} \right\} \right\} \quad (8) \\
 & + \sum_{v=1}^h \{ e_{1v}\rho^v \cos(v\theta) + e_{2v}\rho^v \sin(v\theta) + e_{3v}z\rho^v \cos(v\theta) + e_{4v}z\rho^v \sin(v\theta) \}
 \end{aligned}$$

$$\begin{aligned}
 U = & a + \bar{a} \ln \rho + \sum_{k=1}^g \{ \bar{c}_{3k} \cos(kz)K_0(k\rho) + \bar{c}_{4k} \sin(kz)K_0(k\rho) \\
 & + \sum_{v=1}^h \left\{ \begin{aligned} & \bar{d}_{5kv} \cos(v\theta) \cos(kz)K_v(k\rho) + \bar{d}_{6kv} \sin(v\theta) \sin(kz)K_v(k\rho) \\ & + \bar{d}_{7kv} \cos(v\theta) \sin(kz)K_v(k\rho) + \bar{d}_{8kv} \sin(v\theta) \cos(kz)K_v(k\rho) \end{aligned} \right\} \} \quad (9) \\
 & + \sum_{v=1}^h \{ \bar{e}_{1v}\rho^{-v} \cos(v\theta) + \bar{e}_{2v}\rho^{-v} \sin(v\theta) \}
 \end{aligned}$$

$$\begin{aligned}
 U = & a + bz + \sum_{k=1}^g \left\{ c_{1k} \cosh(kz)J_0(k\rho) + c_{2k} \sinh(kz)J_0(k\rho) \right. \\
 & \left. + c_{3k} \cos(kz)I_0(k\rho) + c_{4k} \sin(kz)I_0(k\rho) \right. \\
 & \left. + \sum_{v=1}^h \left\{ \begin{aligned} & d_{1kv} \cos(v\theta) \cosh(kz)J_v(k\rho) + d_{2kv} \sin(v\theta) \sinh(kz)J_v(k\rho) \\ & + d_{3kv} \cos(v\theta) \sinh(kz)J_v(k\rho) + d_{4kv} \sin(v\theta) \cosh(kz)J_v(k\rho) \\ & + d_{5kv} \cos(v\theta) \cos(kz)I_v(k\rho) + d_{6kv} \sin(v\theta) \sin(kz)I_v(k\rho) \\ & + d_{7kv} \cos(v\theta) \sin(kz)I_v(k\rho) + d_{8kv} \sin(v\theta) \cos(kz)I_v(k\rho) \end{aligned} \right\} \right\} \\
 & + \sum_{v=1}^h \{ e_{1v}\rho^v \cos(v\theta) + e_{2v}\rho^v \sin(v\theta) + e_{3v}z\rho^v \cos(v\theta) + e_{4v}z\rho^v \sin(v\theta) \} \\
 & + \bar{a} \ln \rho + \bar{b}z \ln \rho + \sum_{k=1}^g \left\{ \begin{aligned} & \bar{c}_{1k} \cosh(kz)Y_0(k\rho) + \bar{c}_{2k} \sinh(kz)Y_0(k\rho) \\ & + \bar{c}_{3k} \cos(kz)K_0(k\rho) + \bar{c}_{4k} \sin(kz)K_0(k\rho) \end{aligned} \right\} \\
 & + \sum_{v=1}^h \left\{ \begin{aligned} & \bar{d}_{1kv} \cos(v\theta) \cosh(kz)Y_v(k\rho) + \bar{d}_{2kv} \sin(v\theta) \sinh(kz)Y_v(k\rho) \\ & + \bar{d}_{3kv} \cos(v\theta) \sinh(kz)Y_v(k\rho) + \bar{d}_{4kv} \sin(v\theta) \cosh(kz)Y_v(k\rho) \\ & + \bar{d}_{5kv} \cos(v\theta) \cos(kz)K_v(k\rho) + \bar{d}_{6kv} \sin(v\theta) \sin(kz)K_v(k\rho) \\ & + \bar{d}_{7kv} \cos(v\theta) \sin(kz)K_v(k\rho) + \bar{d}_{8kv} \sin(v\theta) \cos(kz)K_v(k\rho) \end{aligned} \right\} \\
 & + \sum_{v=1}^h \{ \bar{e}_{1v}\rho^{-v} \cos(v\theta) + \bar{e}_{2v}\rho^{-v} \sin(v\theta) + \bar{e}_{3v}z\rho^{-v} \cos(v\theta) + \bar{e}_{4v}z\rho^{-v} \sin(v\theta) \} \quad (10)
 \end{aligned}$$

where k and ν are the order of the T-complete function for approximating the solution. For determining the coefficients of $a, b, c_{1k}, c_{2k}, \dots, \bar{e}_{4\nu}$, we employ the collocation method. Eqs. (8), (9), and (10) can be discretized at a number of collocated points on the Dirichlet boundary. For example, we obtain a system of linear algebraic equations for Eq. (10) as follows:

$$\begin{bmatrix} 1 & z_1 & \cosh(kz_1)J_0(k\rho_1) & \cdots & z_1\rho_1^{-\nu} \sin(\nu\theta_1) \\ 1 & z_2 & \cosh(kz_2)J_0(k\rho_2) & \cdots & z_2\rho_2^{-\nu} \sin(\nu\theta_2) \\ 1 & z_3 & \cosh(kz_3)J_0(k\rho_3) & \cdots & z_3\rho_3^{-\nu} \sin(\nu\theta_3) \\ \vdots & \vdots & \vdots & \ddots & \vdots \\ 1 & z_{aa} & \cosh(kz_{aa})J_0(k\rho_{aa}) & \cdots & z_{aa}\rho_{aa}^{-\nu} \sin(\nu\theta_{aa}) \end{bmatrix} \begin{bmatrix} a \\ b \\ c_{1k} \\ \vdots \\ \bar{e}_{4\nu} \end{bmatrix} = \begin{bmatrix} U_1 \\ U_2 \\ U_3 \\ \vdots \\ U_{aa} \end{bmatrix} \quad (11)$$

Eq. (11) can be written as:

$$\mathbf{A}\mathbf{y} = \mathbf{b}. \quad (12)$$

In Eq. (12), \mathbf{A} is an $aa \times bb$ matrix, \mathbf{y} is a $bb \times 1$ vector, and \mathbf{b} is an $aa \times 1$ vector. Considering the Neumann boundary condition, the collocation method can also be applied. Regarding a problem given in a Cartesian coordinate domain, the flux boundary where the Neumann boundary condition is given can be expressed as

$$U_n = \frac{\partial U}{\partial n} = \nabla U \cdot \mathbf{n} \quad (13)$$

where n denotes the outward normal direction. Using the chain rule, we obtain the expression of $U_x, U_y,$ and U_z in the cylindrical coordinate system. The complete expressions of $U_x, U_y,$ and U_z are listed in Appendix A.

3 Algorithm for solving the ill-posed matrix of the Trefftz method

3.1 The multiple-scale Trefftz method

The accuracy of the numerical solution obtained using the Trefftz method depends sensitively on the distribution of collocated points in satisfying the boundary conditions and particularly on the number of the Trefftz trial functions. Because the resultant system of linear equations is highly ill-conditioned, the numerical solution may be unstable. Hence, we must consider the reduction in the condition number of the resulting linear system.

To mitigate a severely ill-conditioned system of linear equations, this study adopted the multiple scale Trefftz method. According to Liu (2008), the multiple-scale characteristic lengths can significantly reduce condition number of the ill-conditioned

system of linear equations. The multiple-scale characteristic lengths, R_l , can be determined from the \mathbf{A} matrix in Eq. (12) by using

$$R_l = \sqrt{\sum_{i=1}^{aa} A_{i,l}^2}, \quad l = 1, \dots, bb. \tag{14}$$

Using the multiple-scale characteristic lengths, Eq. (8) can be rewritten as

$$\begin{bmatrix} \frac{1}{R_1} & \frac{z_1}{R_2} & \frac{\cosh(kz_1)J_0(k\rho_1)}{R_3} & \dots & \frac{z_1\rho_1^{-\nu} \sin(\nu\theta_1)}{R_{bb}} \\ \frac{1}{R_1} & \frac{z_2}{R_2} & \frac{\cosh(kz_2)J_0(k\rho_2)}{R_3} & \dots & \frac{z_2\rho_2^{-\nu} \sin(\nu\theta_2)}{R_{bb}} \\ \frac{1}{R_1} & \frac{z_3}{R_2} & \frac{\cosh(kz_3)J_0(k\rho_3)}{R_3} & \dots & \frac{z_3\rho_3^{-\nu} \sin(\nu\theta_3)}{R_{bb}} \\ \vdots & \vdots & \vdots & \ddots & \vdots \\ \frac{1}{R_1} & \frac{z_{aa}}{R_2} & \frac{\cosh(kz_{aa})J_0(k\rho_{aa})}{R_3} & \dots & \frac{z_{aa}\rho_{aa}^{-\nu} \sin(\nu\theta_{aa})}{R_{bb}} \end{bmatrix} \begin{bmatrix} a^* \\ b^* \\ c_{1k}^* \\ \vdots \\ \bar{e}_{4\nu}^* \end{bmatrix} = \begin{bmatrix} U_1 \\ U_2 \\ U_3 \\ \vdots \\ U_{aa} \end{bmatrix}. \tag{15}$$

When the above scales R_l in Eq. (14) are used, the condition number of the system of linear equations is greatly reduced. Instead of solving for $[a \ b \ c_{1k} \ \dots \ \bar{e}_{4\nu}]^T$ in Eq. (11), we must solve for the unknown coefficients $[a^* \ b^* \ c_{1k}^* \ \dots \ \bar{e}_{4\nu}^*]^T$ in the multiple scale Trefftz method. In Eq. (15), $R_l, l = 1, \dots, bb$, are the multiple-scale characteristic lengths. We can then rewrite Eq. (15) as:

$$\mathbf{B}\mathbf{x} = \mathbf{b}. \tag{16}$$

where

$$\mathbf{B} = \begin{bmatrix} \frac{1}{R_1} & \frac{z_1}{R_2} & \frac{\cosh(kz_1)J_0(k\rho_1)}{R_3} & \dots & \frac{z_1\rho_1^{-\nu} \sin(\nu\theta_1)}{R_{bb}} \\ \frac{1}{R_1} & \frac{z_2}{R_2} & \frac{\cosh(kz_2)J_0(k\rho_2)}{R_3} & \dots & \frac{z_2\rho_2^{-\nu} \sin(\nu\theta_2)}{R_{bb}} \\ \frac{1}{R_1} & \frac{z_3}{R_2} & \frac{\cosh(kz_3)J_0(k\rho_3)}{R_3} & \dots & \frac{z_3\rho_3^{-\nu} \sin(\nu\theta_3)}{R_{bb}} \\ \vdots & \vdots & \vdots & \ddots & \vdots \\ \frac{1}{R_1} & \frac{z_{aa}}{R_2} & \frac{\cosh(kz_{aa})J_0(k\rho_{aa})}{R_3} & \dots & \frac{z_{aa}\rho_{aa}^{-\nu} \sin(\nu\theta_{aa})}{R_{bb}} \end{bmatrix}, \quad \mathbf{x} = \begin{bmatrix} a^* \\ b^* \\ c_{1k}^* \\ \vdots \\ \bar{e}_{4\nu}^* \end{bmatrix}, \quad \mathbf{b} = \begin{bmatrix} U_1 \\ U_2 \\ U_3 \\ \vdots \\ U_{aa} \end{bmatrix}. \tag{17}$$

In Eq. (17), \mathbf{B} is an $aa \times bb$ matrix, \mathbf{x} is a $bb \times 1$ vector, and \mathbf{b} is an $aa \times 1$ vector. For solving Eq. (16), we multiply \mathbf{B}^T on both sides to form an $n \times n$ system of Eq. (16) as

$$\mathbf{B}^T\mathbf{B}\mathbf{x} = \mathbf{B}^T\mathbf{b}. \tag{18}$$

Eq. (18) can be written as

$$\mathbf{C}\mathbf{x} = \mathbf{D} \tag{19}$$

where $\mathbf{C} = \mathbf{B}^T \mathbf{B}$ is an $bb \times bb$ matrix, \mathbf{x} is the unknown coefficients that is an $bb \times 1$ vector, and $\mathbf{D} = \mathbf{B}^T \mathbf{b}$ is an $bb \times 1$ vector. Generally, linear algebraic equation systems are severely ill-conditioned if k and v increase in value. This becomes an obstacle in solving three-dimensional Laplacian problems by using the CTM. To evaluate whether a given nonsingular matrix is ill-conditioned, we used the condition number in this study. The condition number of the square nonsingular matrix \mathbf{C} is defined by

$$\text{Cond}(\mathbf{C}) = \|\mathbf{C}\| \cdot \|\mathbf{C}^{-1}\| \quad (20)$$

where the matrix norm is the Frobenius norm. If the \mathbf{C} matrix is singular, the condition number is infinite. The detailed study of the multiple-scale Trefftz method for solving three-dimensional Laplacian problems are given in section 4. Since the condition number of the system of linear equations is greatly reduced by using the multiple-scale Trefftz method, we can then apply the DJIFM for solving the linear system. The DJIFM is described in the following section.

3.2 The Dynamical Jacobian-Inverse Free Method (DJIFM)

In recent years, various contributions toward the numerical solutions of linear algebraic equations have been made. An iterative-based method such as the conjugate gradient method (CGM) [Liu, Hong, and Atluri, (2010)] is perhaps the best-known technique for determining successively enhanced approximations to the solutions of a system of linear algebraic equations. That the convergence of the CGM depends on the eigenvalue distribution of a system of linear algebraic equations is well-known. When a linear algebraic equation system is typically extremely ill-conditioned, the convergence of the CGM can be unacceptably slow or may be unable to converge [Vuik, Segal, and Meijerink (1999)].

In addition to the CGM, the Fictitious Time Integration Method (FTIM) was first used to solve a nonlinear system of algebraic equations by introducing fictitious time [Liu and Atluri (2008); Ku, Yeih, Liu, and Chi (2009)]. Inspired by the FTIM, the DJIFM from the general dynamical method [Ku, Yeih, and Liu (2010); Ku and Yeih (2012)] has been proposed using a scalar homotopy function to transform a vector function of linear or non-linear algebraic equations into a time-dependent scalar function by introducing a fictitious time-like variable. This demonstrated great numerical stability for solving linear or non-linear algebraic equations, particularly for systems involving ill-conditioned Jacobian or poor initial values that cause convergence problems. Accordingly, we adopted the DJIFM for mitigating the ill-conditioned systems of linear algebraic equations in this study. The system of linear equations for solving the three-dimensional Laplacian problems by using

the CTM, as shown in Eq. (16), can be rewritten as

$$\mathbf{F}(\mathbf{x}) = \mathbf{C}\mathbf{x} - \mathbf{D} = \mathbf{0} \tag{21}$$

The general dynamical equation for solving linear algebraic equations can be expressed as

$$\dot{\mathbf{x}} = -\frac{\dot{Q}(t)}{2Q(t)} \frac{\|\mathbf{F}(\mathbf{x})\|^2}{\mathbf{F}^T(\mathbf{x})\mathbf{B}\mathbf{F}(\mathbf{x})} \mathbf{F}(\mathbf{x}). \tag{22}$$

Based on the general dynamical method, the $Q(t)$ in the above equation is a monotonically increasing function of t and it must satisfy the conditions that $Q(t) > 0$ and $Q(0) = 1$. A suitable function of $Q(t)$ can be easily found as $Q(t) = e^t$. Accordingly, we have $\dot{Q}(t)/Q(t) = 1$. Eq. (19) can be rewritten as

$$\dot{\mathbf{x}} = -\frac{1}{2} \frac{\|\mathbf{F}(\mathbf{x})\|^2}{\mathbf{F}^T(\mathbf{x})\mathbf{B}\mathbf{F}(\mathbf{x})} \mathbf{F}(\mathbf{x}). \tag{23}$$

If we let the transformation matrix, \mathbf{T} , be the identity matrix, \mathbf{I} , then Eq. (23) becomes the DJIFM and can be written as

$$\dot{\mathbf{x}} = -\frac{1}{2} \frac{\|\mathbf{F}(\mathbf{x})\|^2}{\mathbf{F}^T(\mathbf{x})\mathbf{B}\mathbf{F}(\mathbf{x})} \mathbf{F}(\mathbf{x}). \tag{24}$$

In Eq. (24), \mathbf{B} is a Jacobian matrix of $\mathbf{F}(\mathbf{x})$. Because $\mathbf{F}(\mathbf{x})$ is a system of linear algebraic equations, \mathbf{B} is simply equal to the \mathbf{C} matrix in this study. In using Eq. (24), we may employ a forward Euler scheme and obtain the following equations:

$$\mathbf{x}^{k+1} = \mathbf{x}^k - \frac{h_t}{2} \frac{\|\mathbf{F}(\mathbf{x}^k)\|^2}{\mathbf{F}^T(\mathbf{x}^k)\mathbf{B}(\mathbf{x}^k)\mathbf{F}(\mathbf{x}^k)} \mathbf{F}(\mathbf{x}^k). \tag{25}$$

In the above equation h_t is the fictitious time step. The numerator and denominator of the fraction in this equation are scalars. Accordingly, we can avoid computing the inverse of the Jacobian matrix, thus improving numerical stability. Because the condition number of the \mathbf{C} matrix has been reduced, the system of linear algebraic equations, $\mathbf{C}\mathbf{x} - \mathbf{D} = 0$, can be solved yielding an extremely high accuracy. In addition, the limitation of convergence for solving the ill-conditioned linear algebraic equations can also be released.

4 Numerical examples

4.1 Example 1

The first scenario investigated is a three-dimensional homogenous isotropic groundwater flow problem [Strack (1989)]. With a three-dimensional simply connected

domain Ω enclosed by boundary, the Laplace governing equation is expressed as

$$\nabla^2 u = 0 \quad \text{in } \Omega. \quad (26)$$

An object domain under consideration Ω is defined as

$$\Omega = \{(x, y, z) | x = r \sin \theta \cos \phi, y = r \sin \theta \sin \phi, z = r \cos \theta\}. \quad (27)$$

where $r = 2$, $0 \leq \theta \leq 2\pi$, $0 \leq \phi \leq \pi$.

The analytical solution is given by

$$u = e^y \cos x + e^x \sin z. \quad (28)$$

The Dirichlet boundary condition is given on the boundaries by using the analytical solution for the problem as shown in Eq. (28). In this example, 2106 boundary collocation points were uniformly placed on the entire boundary, as depicted in Fig. 3. Figure 4 shows that the relationship of the condition number versus the order of v and k after using the CTM and the multiple scale Trefftz method. It is found that the condition number increases with v and k and the maximum condition number is 1.74×10^{48} for the CTM when $v = k = 20$. However, it is also interesting to find that the condition number remains in the order of 10^{19} after v and k greater than six for the multiple scale Trefftz method. It is obvious that the multiple scale Trefftz method can effectively reduce the condition number of the system of linear equations. It is also demonstrated that no any available methods can be used to solve the severely ill-conditioned system if we use the CTM for solving this three-dimensional problem.

Using the multiple scale Trefftz method, the condition number of the system of linear equations is 2.71×10^{18} for $v = k = 12$. Although the condition number is greatly reduced, it is still too ill-conditioned to solve for most of the linear equation solvers. To overcome this difficulty, we adopted the DJIFM to solve this three-dimensional Laplacian problem. The root mean square norm of 1.00×10^{-8} is set as the stopping criterion. The fictitious time step h_t in the DJIFM is assumed to be 1. To demonstrate the capability of the DJIFM for dealing with the ill-conditioned system of linear equations, the CGM was adopted for the comparison. Figure 5 shows the convergence of the DJIFM as well as the CGM. The number of fictitious steps is about 1.5×10^5 to reach the stopping criterion for the DJIFM. However, it is found that the CGM is not able to converge to the preset stopping criterion due to the severely ill-conditioned system. To view the results clearly, the computed data were projected onto xy and xz planes and were compared with the analytical solution on the internal 8000 collocation points as shown in Fig. 6 and Fig. 7. It is found that the maximum error was less than 5.00×10^{-5} and that the numerical solution agreed well with the analytical solution.

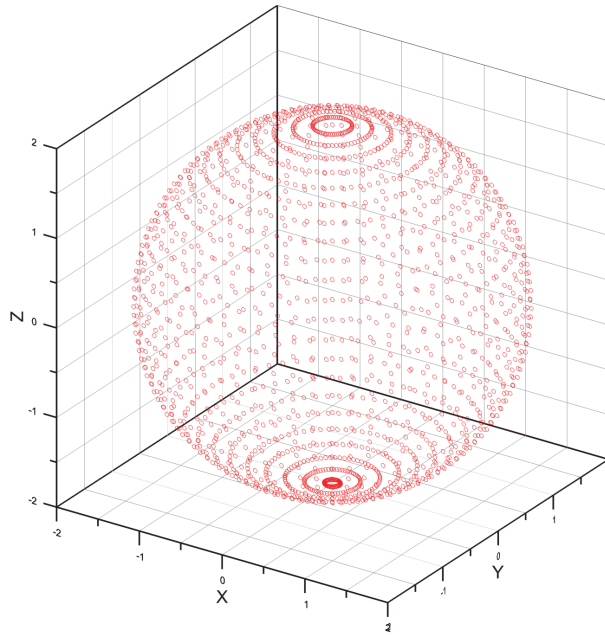


Figure 3: A simply connected domain and total 2106 boundary collocation points for the analysis of example 1.

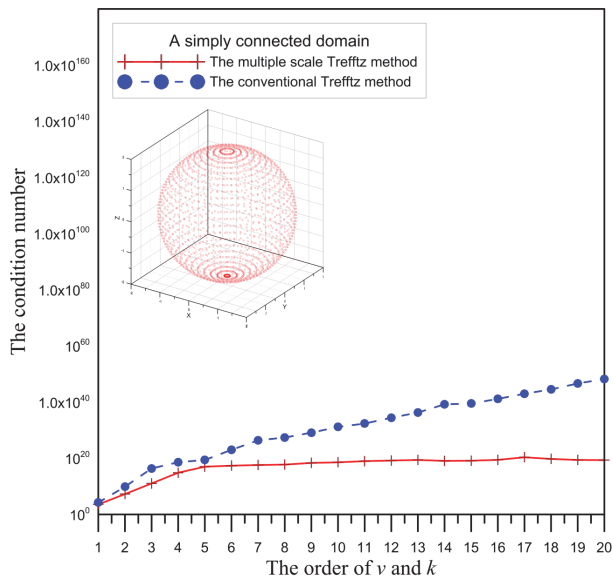


Figure 4: The condition number versus the order of ν and k for example 1.

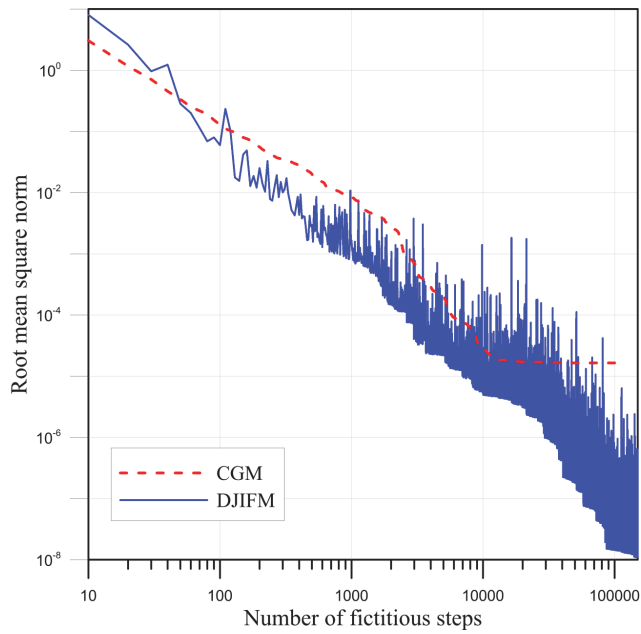


Figure 5: Convergence of the DJIFM for example 1.

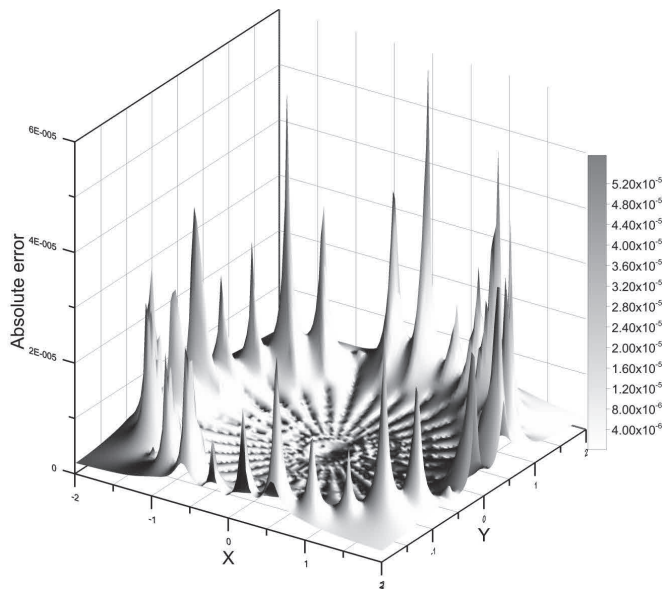


Figure 6: Absolute error of the computed results with exact solution for example 1. (projected in xy plane)

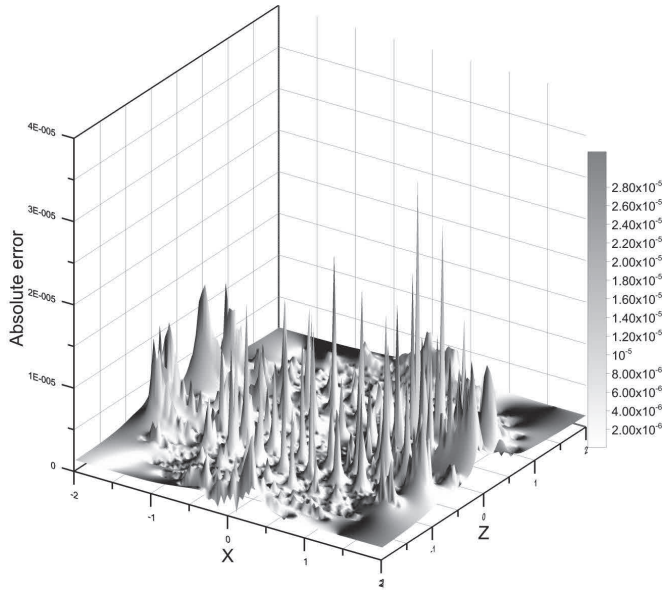


Figure 7: Absolute error of the computed results with exact solution for example 1. (projected in xz plane)

4.2 Example 2

The second example investigated was a three-dimensional homogenous isotropic groundwater flow problem in an infinite domain with a cavity. The example is usually referred as an exterior problem. The cavity is enclosed by a cylinder-type boundary as shown in Fig. 8 the Laplace governing equation is expressed as

$$\nabla^2 u = 0 \quad \text{in } \Omega. \tag{29}$$

The object domain under consideration Ω is an infinite domain with a cavity. The boundary of the cavity is defined as

$$\Gamma = \{(x, y, z) \mid x = \rho \cos \theta, \ y = \rho \sin \theta, \ -1 \leq z \leq 1\}. \tag{30}$$

where $\rho = 1.2$ and $0 \leq \theta \leq 2\pi$.

The analytical solution of the problem is given as

$$u = \frac{1}{\sqrt{x^2 + y^2 + z^2}}. \tag{31}$$

The Dirichlet boundary condition is given on the boundary of the cavity by using the analytical solution for the problem as shown in Eq. (31). In this example,

the total 4896 boundary collocation points were uniformly placed on the entire boundary as shown in Fig. 8. Figure 9 shows that the relationship of the condition number versus the order of ν and k after using the CTM and the multiple scale Trefftz method. The maximum condition number is 2.95×10^{112} for the CTM when $\nu = k = 20$. It is noted that the condition number remains in the order of 10^{19} after ν and k greater than six for the multiple scale Trefftz method.

Using the multiple scale Trefftz method, the condition number of the system of linear equations is 3.83×10^{20} for $\nu = k = 20$. We adopted the DJIFM to solve the three-dimensional Laplacian problem by using the multiple scale Trefftz method. Both the root mean square norm of 1.00×10^{-6} and the maximum number of 5×10^5 fictitious steps were set as the stopping criterion. The fictitious time step h_t in the DJIFM was assumed to be one. In this example, the maximum number of fictitious steps was first reached. Because this example is an interior problem, we selected a ring outside the cylinder for comparing the results. The computed results were compared with the analytical solution as shown in Fig. 10. It is found that the maximum error was less than 3.00×10^{-3} and that the numerical solution agreed well with the analytical solution.

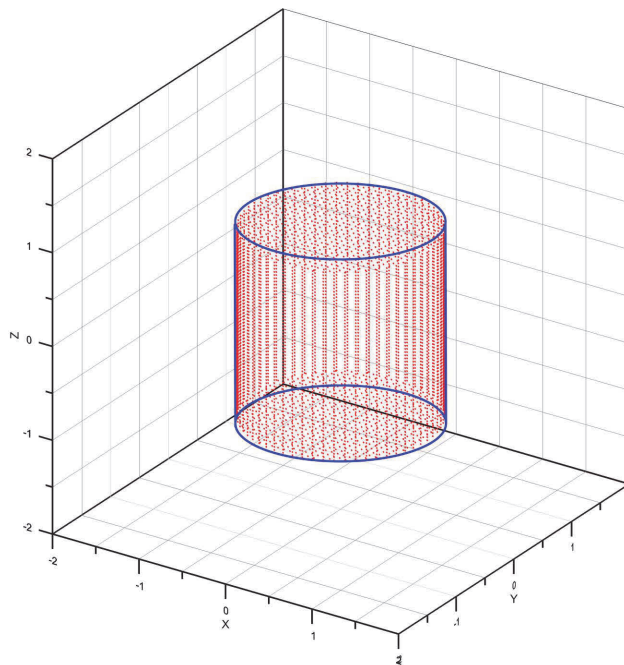


Figure 8: An infinite domain with a cavity and total 4896 boundary collocation points for the analysis of example 2.

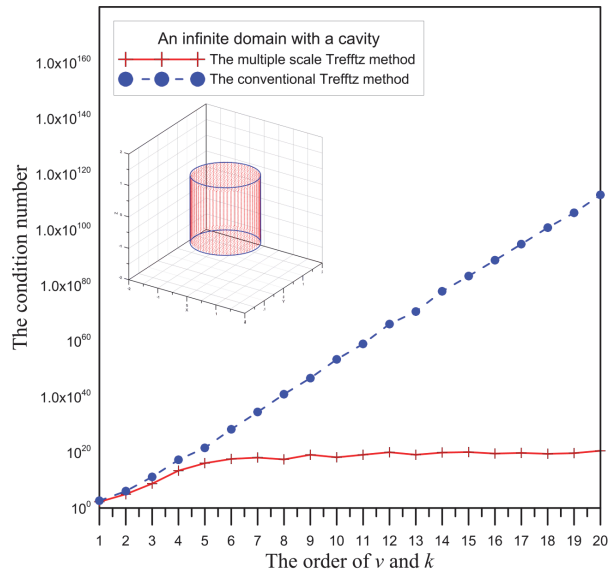


Figure 9: The condition number versus the order of ν and k for example 2.

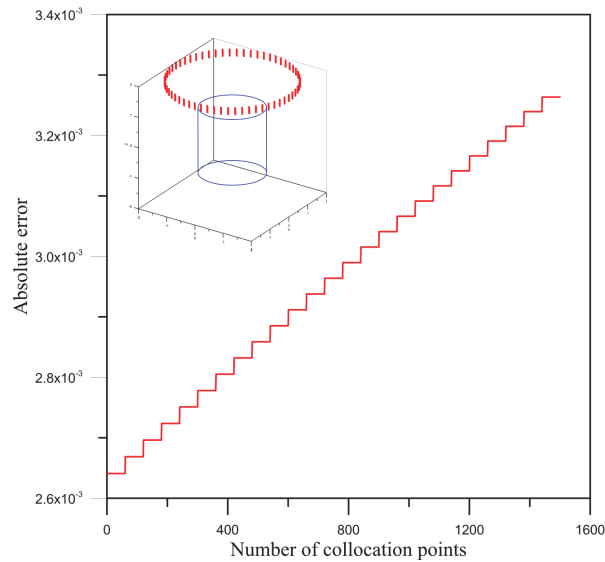


Figure 10: Absolute error of the computed results with exact solution for example 2.

4.3 Example 3

The third example investigated was a three-dimensional homogenous isotropic ground-water flow problem with an imperious cylinder in a domain. In this example, we solved the boundary value problem with the Dirichlet boundary data and the Neumann boundary data. With a three-dimensional doubly connected domain Ω enclosed by boundary, as shown in Fig. 11, the Laplace governing equation is expressed as

$$\nabla^2 u = 0 \quad \text{in } \Omega. \quad (32)$$

An object domain under consideration Ω is defined as

$$\Omega \in \{-6 \leq x \leq 6, -6 \leq y \leq 6, -6 \leq z \leq 6\}. \quad (33)$$

The boundary of the internal cylinder is defined as

$$\Gamma = \{(x, y, z) \mid x = \rho \cos \theta, y = \rho \sin \theta, -6 \leq z \leq 6\}. \quad (34)$$

where $\rho = 2.23$ and $0 \leq \theta \leq 2\pi$.

The analytical solution of the problem is given as

$$u = xyz. \quad (35)$$

The Dirichlet boundary and the Neumann boundary conditions as shown in Fig. 12 are given on the boundaries by using the analytical solution for the problem. Therefore, the Dirichlet boundary condition with the analytical solution for $u = xyz$ is applied to Γ_{D1} and Γ_{D2} as

$$\Gamma_{D1} = \{(x, y, z) \mid x = \pm 6, -6 \leq y \leq 6, -6 \leq z \leq 6\}. \quad (36)$$

$$\Gamma_{D2} = \{(x, y, z) \mid -6 \leq x \leq 6, -6 \leq y \leq 6, z = \pm 6\}. \quad (37)$$

The Neumann boundary condition with the analytical solution of $u_n = xz$ is applied to

$$\Gamma_N \quad \text{where} \quad \Gamma_N = \{(x, y, z) \mid -6 \leq x \leq 6, y = \pm 6, -6 \leq z \leq 6\}. \quad (38)$$

In this example, 18168 boundary collocation points were uniformly placed on the entire boundary, as depicted in Fig. 11 Figure 13 shows that the relationship of the condition number versus the order of v and k after using the CTM and the multiple scale Trefftz method. The maximum condition number is 4.78×10^{165} for the CTM when $v = k = 20$. It is noted that the condition number remains in the order of 10^{20} after v and k greater than eight for the multiple scale Trefftz method.

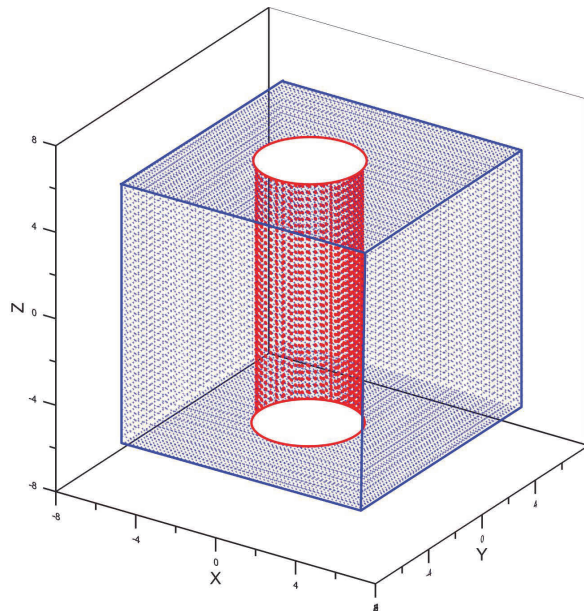


Figure 11: A doubly connected domain and total 18168 boundary collocation points for the analysis of example 3.

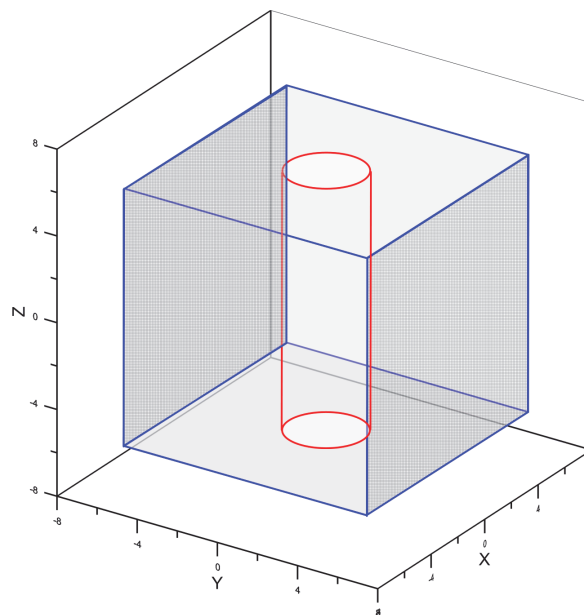


Figure 12: A doubly connected domain with the Neumann boundary condition (the dark area) for the analysis of example 3.

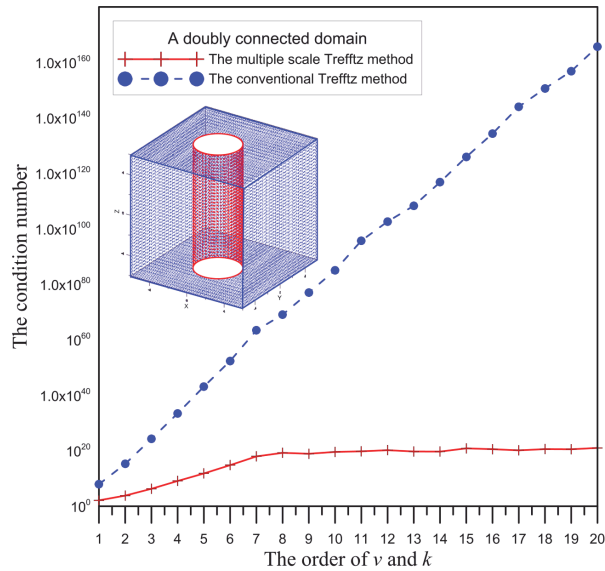


Figure 13: The condition number versus the order of ν and k for example 3.

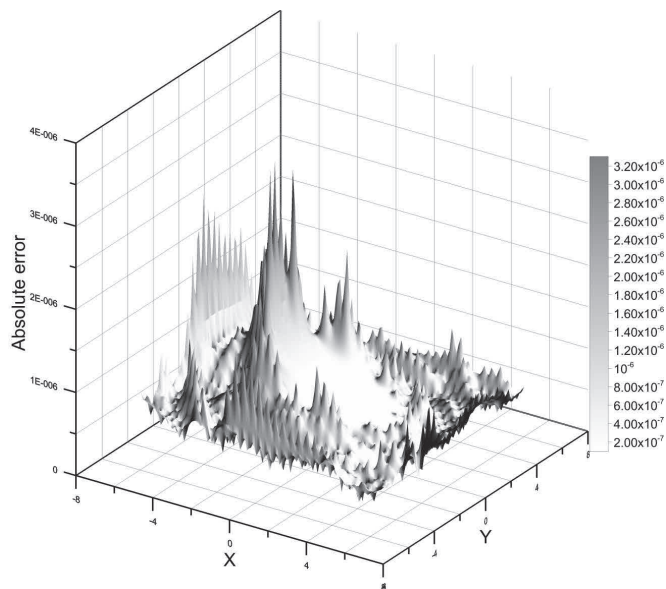


Figure 14: Absolute error of the computed results with exact solution for example 3. (projected in xy plane)

Using $\nu = k = 6$, we adopted the DJIFM to solve the three-dimensional Laplacian problem by using the multiple scale Trefftz method. The root mean square norm of 1.00×10^{-7} is set as the stopping criterion. The computed data were projected onto an xy plane and were compared with the analytical solution as shown in Fig 14. It is found that the maximum error was less the 3.0×10^{-6} and that the numerical solution agreed very well with the analytical solution.

4.4 Example 4

Dong and Atluri (2012) developed 3D T-Trefftz Voronoi cell finite elements with/without spherical voids &/or elastic/rigid inclusions for micromechanical modeling of heterogeneous materials. It is interesting to investigate a three-dimensional homogenous isotropic groundwater flow problem with an imperious spherical void in a domain. Therefore, in this example we solved the boundary value problem with the Dirichlet boundary data and the Neumann boundary data. With a three-dimensional doubly connected domain Ω enclosed by boundary, as shown in Fig. 15 the Laplace governing equation is expressed as

$$\nabla^2 u = 0 \quad \text{in } \Omega. \quad (39)$$

An object domain under consideration Ω is defined as

$$\Omega \in \{-2 \leq x \leq 2, -2 \leq y \leq 2, -2 \leq z \leq 2\}. \quad (40)$$

The boundary of the internal sphere is defined as

$$\Gamma = \{(x, y, z) \mid x = \rho \cos \zeta \sin \xi, y = \rho \sin \zeta \sin \xi, z = \rho \cos \xi\}. \quad (41)$$

where $\rho = 1$, $-\pi/2 \leq \zeta \leq \pi/2$, and $-\pi \leq \xi \leq \pi$.

The analytical solution of the problem is given as

$$u = xyz. \quad (42)$$

Both of the Dirichlet boundary and the Neumann boundary data are applied on 2168 collocation points of six identical square faces of the cubic domain. The Dirichlet boundary data are applied on 2016 collocation points of the internal surface of the sphere, as depicted in Fig. 15 To study the effect of the order of ν and k , we only used $\nu = k = 2$. In this particular example, the condition number is about 1.47×10^{17} . Because it is not very ill-conditioned system, we adopted the commercial program MATLAB backslash operator to solve a system of simultaneous linear equations.

The internal 9000 collocation points were placed inside the cubic domain. To view the results clearly, the profiles on $x = 0$ and $y = 0$ were selected to compare with the

analytical solution. The computed data on $x = 0$ and $y = 0$ profiles were projected onto yz and xz planes and were compared with the analytical solution as shown in Fig 16 and Fig. 17. It is found that the maximum error was less the 3.0×10^{-15} and that the numerical solution agreed very well with the analytical solution.

Dong and Atluri (2012) developed 3D Trefftz Voronoi cells with ellipsoidal voids &/or elastic/rigid inclusions for micromechanical modeling of heterogeneous materials. To further investigate the effect of the geometry in this study, we conducted this example again. Considering this problem with an imperious ellipsoidal in a domain as shown in Fig. 18 other conditions are remained exactly the same as the previous one. The boundary of the internal ellipsoidal is defined as

$$\Gamma = \{(x, y, z) \mid x = \rho_a \cos \zeta \cos \xi, y = \rho_b \cos \zeta \sin \xi, z = \rho_c \sin \zeta\}. \tag{43}$$

where $\rho_a = 1.8, \rho_b = 1.0, \rho_c = 0.8, -\pi \leq \zeta \leq \pi$, and $-\pi/2 \leq \xi \leq \pi/2$.

Again, to study the effect of the order of v and k , we only used $v = k = 3$. In this example, the condition number is about 1.06×10^5 . Because it is not ill-conditioned system, we adopted the commercial program MATLAB backslash operator to solve a system of simultaneous linear equations.

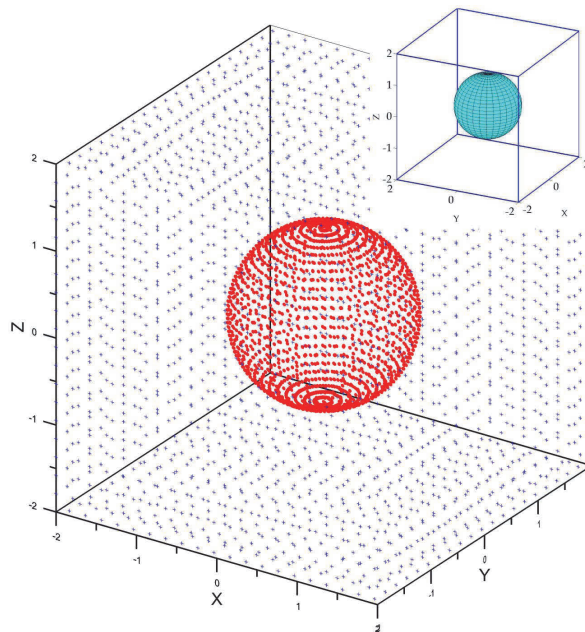


Figure 15: A doubly connected domain with a spherical cavity for the analysis of example 4.

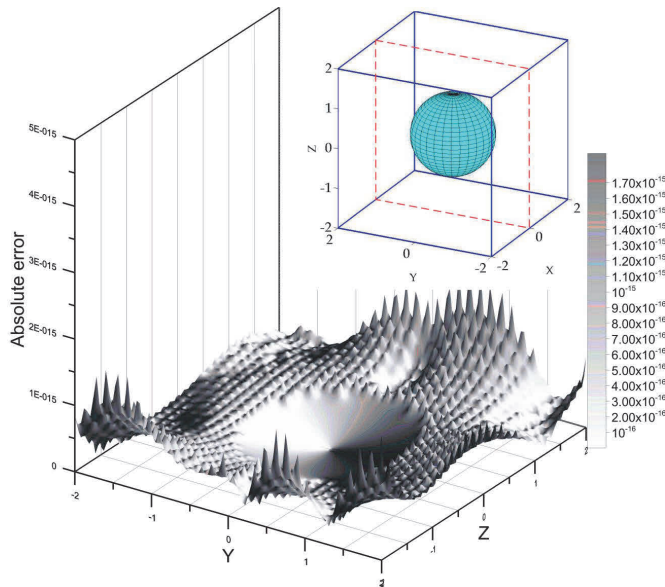


Figure 16: Absolute error of the computed results with exact solution on $x = 0$ slice for example 4. (projected in yz plane)

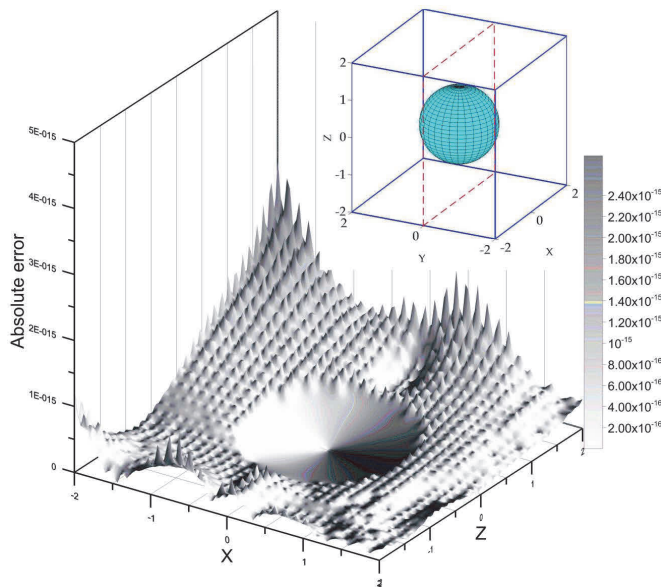


Figure 17: Absolute error of the computed results with exact solution on $y = 0$ slice for example 4. (projected in xz plane)

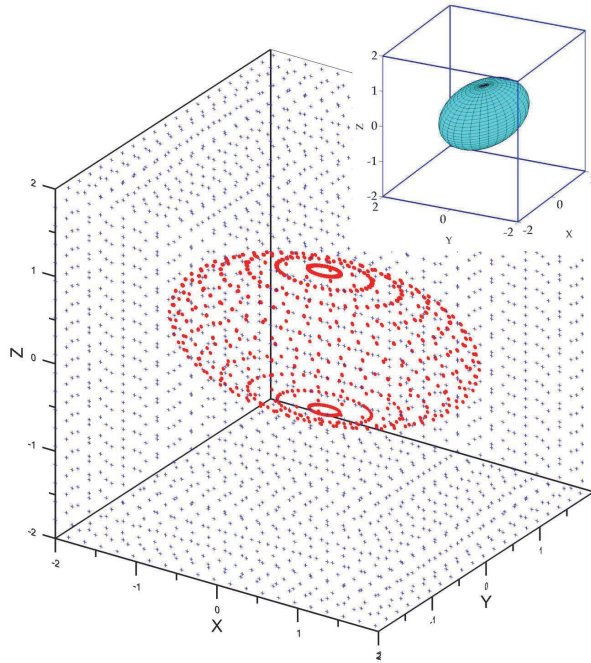


Figure 18: A doubly connected domain with an ellipsoidal cavity for the analysis of example 4.

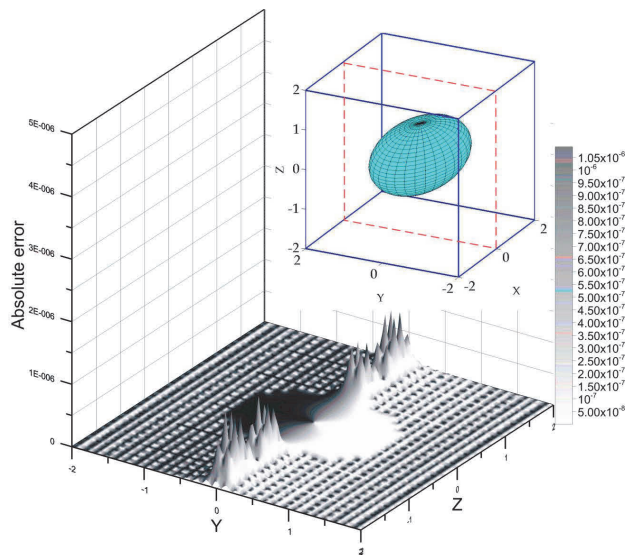


Figure 19: Absolute error of the computed results with exact solution on $x = 0$ slice for example 4. (projected in yz plane)

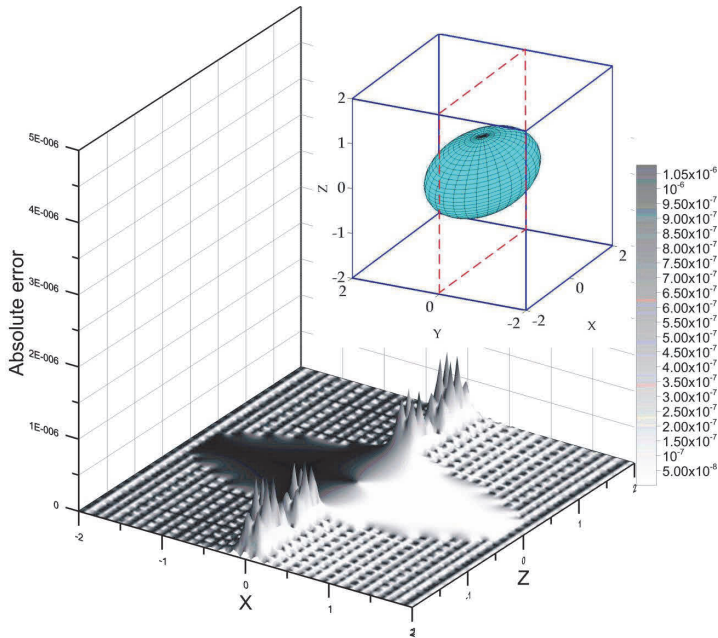


Figure 20: Absolute error of the computed results with exact solution on $y = 0$ slice for example 4. (projected in xz plane)

The internal 9000 collocation points were placed inside the cubic domain. To view the results clearly, the profiles on $x = 0$ and $y = 0$ were selected to compare with the analytical solution. The computed data on $x = 0$ and $y = 0$ profiles were projected onto yz and xz planes and were compared with the analytical solution as shown in Fig 19 and Fig. 20. It is found that the maximum error was less the 2.0×10^{-6} and that the numerical solution agreed very well with the analytical solution This example also demonstrates that the proposed method can obtain accurate numerical solutions with ν and k in very low order.

4.5 Example 5

The last example investigated was a three-dimensional homogenous isotropic groundwater flow problem with two imperious cylinders in a domain, as shown in Fig. 21. With a three-dimensional multiply connected domain Ω enclosed by boundary, the Laplace governing equation is expressed as

$$\nabla^2 u = 0 \quad \text{in } \Omega. \tag{44}$$

An object domain under consideration Ω is defined as

$$\Omega \in \{-4 \leq x \leq 4, -4 \leq y \leq 4, -4 \leq z \leq 4\}. \quad (45)$$

The center of the first cylinder is $(x_1, y_1, z_1) = (0, 0, 0)$ and the boundary is defined as

$$\Gamma_1 = \{(x, y, z) \mid x = x_1 + \rho_1 \cos \theta_1, y = y_1 + \rho_1 \sin \theta_1, -4 \leq z \leq 4\} \quad (46)$$

where $\rho_1 = 1$ and $0 \leq \theta_1 \leq 2\pi$.

The center of the second cylinder is $(x_2, y_2, z_2) = (2, 2, 0)$ and the boundary is defined as

$$\Gamma_2 = \{(x, y, z) \mid x = x_2 + \rho_2 \cos \theta_2, y = y_2 + \rho_2 \sin \theta_2, -4 \leq z \leq 4\} \quad (47)$$

where $\rho_2 = 1.2$ and $0 \leq \theta_2 \leq 2\pi$.

The analytical solution of the problem is given as

$$u = \frac{z \cos \theta_{i1}}{\rho_{i1}} + \frac{z \cos \theta_{i2}}{\rho_{i2}}, \quad (48)$$

where $\rho_{i1} = \sqrt{(x - x_1)^2 + (y - y_1)^2}$, $\theta_{i1} = \arctan\left(\frac{y - y_1}{x - x_1}\right)$ and

$$\rho_{i2} = \sqrt{(x - x_2)^2 + (y - y_2)^2}, \quad \theta_{i2} = \arctan\left(\frac{y - y_2}{x - x_2}\right). \quad (49)$$

The Dirichlet boundary condition is given on the boundaries by using the analytical solution for the problem, as shown in Eq. (48). In this example, 4808 boundary collocation points were uniformly placed on the entire boundary, as depicted in Fig. 21. Figure 22 shows that the relationship of the condition number versus the order of v and k after using the CTM and the multiple scale Trefftz method. The maximum condition number is 1.09×10^{122} for the CTM when $v = k = 20$. It is noted that the condition number remains in the order of 10^{20} after v and k greater than six for the multiple scale Trefftz method.

Using $v = k = 9$, we adopted the DJIFM to solve the three-dimensional Laplacian problem by using the multiple scale Trefftz method. The root mean square norm of 1.00×10^{-6} is set as the stopping criterion. The computed data were projected onto an xy plane and were compared with the analytical solution as shown in Fig 23. It is found that the maximum error was less the 1.4×10^{-3} and that the numerical solution agreed very well with the analytical solution.

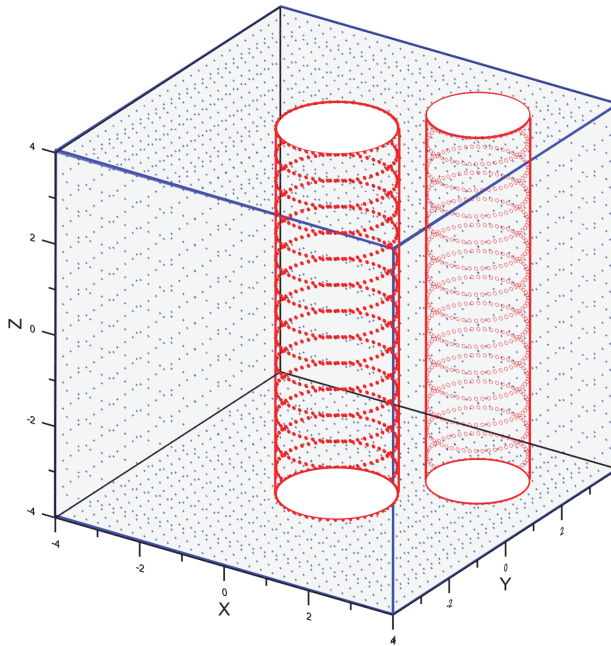


Figure 21: A multiply connected domain and total 4808 boundary collocation points for the analysis of example 5.

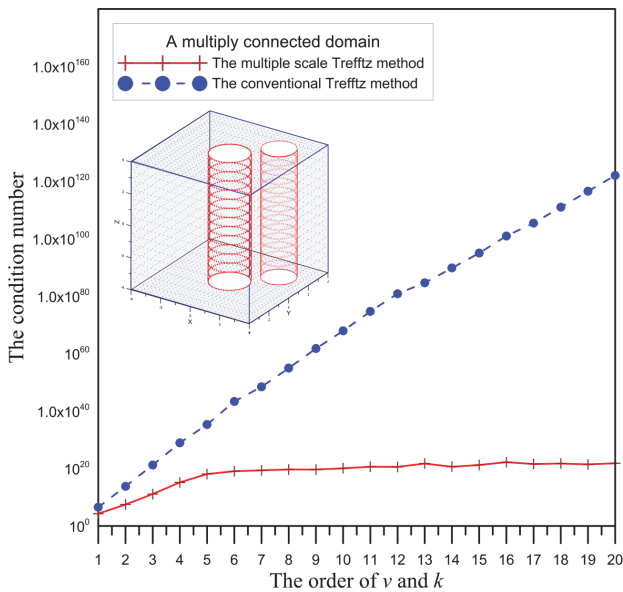


Figure 22: The condition number versus the order of ν and k for example 5.

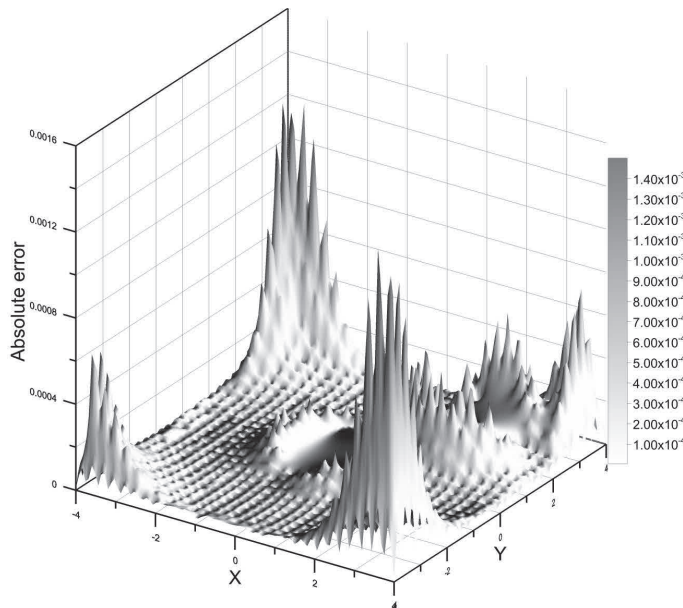


Figure 23: Absolute error of the computed results with exact solution for example 5. (projected in xy plane)

5 Conclusion

This study proposes a numerical solution for three-dimensional Laplacian problems in a multiply connected domain approximated with the T-complete function and formulated using 36 functions in the cylindrical coordinate system. The fundamental concepts and the construct of the proposed method are addressed in detail. The findings are addressed as follows:

The Trefftz formulation based on the cylindrical coordinate system for the numerical solution of three-dimensional Laplacian problems in a multiply connected domain was first successfully developed. The basis for the T-complete function including 36 functions was derived. Numerical solutions including three-dimensional groundwater flow problems in a simply connected domain, an infinite domain, a doubly connected domain, and a multiply connected domain demonstrate the proposed method can be used to deal with complicated three-dimensional engineering problems with great ease.

Due to the adoption of the generalized multiple source point boundary collocation Trefftz method, the complicated three-dimensional problems in a multiply connected domain can be tackled without introducing the decomposition of the prob-

lem domain. The advantage of the proposed method can be used to deal with more complicated three-dimensional object domain in the future.

The resulting system of linear equations based on the conventional CTM is typically extremely ill-conditioned. The obstacle for the solution of three-dimensional Laplacian problems by the collocation Trefftz method was successfully overcome by the multiple scale Trefftz method and the DJIFM. The results revealed that the proposed method can obtain accurate numerical solutions for three-dimensional Laplacian problems, yielding a superior convergence in numerical stability to that of the conventional Trefftz method.

Acknowledgement: This study was partially supported by the National Science Council under project grant NSC100-2628-E-019-054-MY3. The author thank the National Science Council for the generous financial support. The author is also grateful to the former student, Shu-Han Wang, for his assistance of this study.

References

- Chen, C. S.; Cho, Hokwon A; Golberg, M. A.** (2006): Some comments on the ill-conditioning of the method of fundamental solutions. *Eng Anal Bound Elem*, vol. 30, pp. 405-410.
- Chen, J. T.; Wu, C. S.; Lee, Y. T.; Chen, K. H** (2007): On the equivalence of the Trefftz method and method of fundamental solutions for Laplace and biharmonic equations. *Computers and Mathematics with Applications*, vol. 53, pp. 851-879.
- Dong, L.; Atluri, S. N.** (2012): A simple multi-source-point Trefftz method for solving direct/inverse SHM problems of plane elasticity in arbitrary multiply - connected domains. *CMES-Comp Model Eng*, vol. 85, no. 1, pp. 1-43.
- Dong, L.; Atluri, S. N.** (2012): Development of 3D TTrefftz Voronoi cell finite elements with/without spherical voids &/or elastic/rigid inclusions for micromechanical modeling of heterogeneous materials. *CMC-Comput Mater Con*, vol. 29, no. 2, pp. 169-211.
- Dong, L.; Atluri, S. N.** (2012): Development of 3D Trefftz Voronoi cells with ellipsoidal voids &/or elastic/rigid inclusions for micromechanical modeling of heterogeneous materials. *CMC-Comput Mater Con*, vol. 30, no 1, pp. 39-81.
- Fan, C. M.; Chan, H. F.; Kuo, C. L.; Yeih, W.** (2012): Numerical solutions of boundary detection problems using modified collocation Trefftz method and exponentially convergent scalar homotopy algorithm. *Eng Anal Bound Elem*, vol. 36, pp. 2-8.
- Kita, E; Kamiya, N.** (1995): Trefftz method: an overview. *Adv Eng Softw*, vol.

24, pp. 3-12.

Kita, E.; Kamiya, N.; Iio, T. (1999): Application of a direct Trefftz method with domain decomposition to 2D potential problems. *Eng Anal Bound Elem*, vol. 23, pp. 539-548.

Kita, E.; Ikedab, Y.; Kamiya, N. (2005): Trefftz solution for boundary value problem of three-dimensional Poisson equation. *Eng Anal Bound Elem*, vol. 29, pp. 383-390.

Ku, C. Y.; Yeih, W.; Liu, C. S.; Chi, C. C. (2009): Applications of the fictitious time integration method using a new time-like function. *CMES-Comp Model Eng*, vol. 43, no. 2, pp. 173-190.

Ku, C. Y.; Yeih, W.; Liu, C. S. (2010): Solving Non-Linear Algebraic Equations by a Scalar Newton-homotopy Continuation Method. *Int J Nonlin Sci Num*, vol. 11, no. 6, pp. 435-450.

Ku, C. Y.; Yeih, W. (2012): Dynamical Newton-Like Methods with Adaptive Step-size for Solving Nonlinear Algebraic Equations. *CMC-Comput Mater Con*, vol. 31, no. 3, pp. 173-200.

Ku, C. Y.; Yeih, W.; Liu, C. S. (2011): Dynamical Newton-Like Methods for Solving Ill-Conditioned Systems of Nonlinear Equations with Applications to Boundary Value Problems. *CMES-Comp Model Eng*, vol. 76, no. 2, pp. 83-108.

Li, Z. C.; Lu, Z. Z.; Hu, H. Y.; Cheng, AH-D. (2008): *Trefftz and Collocation Methods*, WIT Press, Southampton/Boston.

Liu, C. S. (2007): A modified Trefftz method for two-dimensional Laplace equation considering the domain's characteristic length. *CMES-Comp Model Eng*, vol. 21, pp. 53-65.

Liu, C. S. (2008): A modified collocation Trefftz method for the inverse Cauchy problem of Laplace equation. *Eng Anal Bound Elem*, vol. 32, pp. 78-85.

Liu, C. S.; Atluri, S. N. (2008): A novel time integration method for solving a large system of non-linear algebraic equations. *CMES-Comp Model Eng*, vol. 31, pp. 71-83.

Liu, C. S.; Hong, H. K.; Atluri, S. N. (2010): Novel Algorithms Based on the Conjugate Gradient Method for Inverting Ill-Conditioned Matrices, and a New Regularization Method to Solve Ill-Posed Linear Systems. *CMES-Comp Model Eng*, vol. 60, pp. 279-308.

Liu, C. S.; Atluri, S. N. (2013): Numerical solution of the Laplacian Cauchy problem by using a better postconditioning collocation Trefftz method. *Eng Anal Bound Elem*, vol. 37, pp. 74-83.

Vuik, C.; Segal, A.; Meijerink J. A. (1999): An Efficient Preconditioned CG

Method for the Solution of a Class of Layered Problems with Extreme Contrasts in the Coefficients. *J Comput Phys*, vol. 152, pp. 385-403.

Strack, O. D.(1989): *Groundwater Mechanics*. Prentice Hall Englewood Cliffs, New Jersey.

Trefftz, E. (1926): *Ein Gegenstück zum Ritzschen Verfahren*. Proc 2nd Int Cong Appl Mech, Zurich; pp. 131-137.

Yeih, W.; Liu, C. S.; Kuo, C. L.; Atluri, S. N. (2010): On solving direct/inverse Cauchy problems of Laplace equation in a multiply connected domain, using the generalized multiple-source-point boundary-collocation Trefftz method & characteristic lengths. *CMES-Comp Model Eng*, vol. 17, no. 3, pp. 275-302.

Appendix A. Complete expressions of U_x, U_y and U_z

If a problem is given in Cartesian coordinates then the chain rule can be applied and the Neumann boundary conditions of $U_x, U_y,$ and U_z can be written as

$$\frac{\partial U}{\partial x} = \frac{\partial U}{\partial \rho} \frac{\partial \rho}{\partial x} + \frac{\partial U}{\partial \theta} \frac{\partial \theta}{\partial x}$$

$$\frac{\partial U}{\partial y} = \frac{\partial U}{\partial \rho} \frac{\partial \rho}{\partial y} + \frac{\partial U}{\partial \theta} \frac{\partial \theta}{\partial y}$$

$$\frac{\partial U}{\partial z}$$

Through a series of mathematical operations, we obtain the expressions of $U_x, U_y,$ and U_z in the cylindrical coordinate system as follows.

$$U_\rho = \sum_{k=1}^g \left\{ \begin{array}{l} -c_{1k}k \cosh(kz)J_1(k\rho) \\ -c_{2k}k \sinh(kz)J_1(k\rho) \\ +c_{3k}k \cos(kz)I_1(k\rho) \\ +c_{4k}k \sin(kz)I_1(k\rho) \end{array} \right. + \sum_{v=1}^h \left\{ \begin{array}{l} d_{1kv}k \cos(v\theta) \cosh(kz)(-J_{v+1}(k\rho) + \frac{v}{k\rho}J_v(k\rho)) \\ +d_{2kv}k \sin(v\theta) \sinh(kz)(-J_{v+1}(k\rho) + \frac{v}{k\rho}J_v(k\rho)) \\ +d_{3kv}k \cos(v\theta) \sinh(kz)(-J_{v+1}(k\rho) + \frac{v}{k\rho}J_v(k\rho)) \\ +d_{4kv}k \sin(v\theta) \cosh(kz)(-J_{v+1}(k\rho) + \frac{v}{k\rho}J_v(k\rho)) \\ +d_{5kv}k \cos(v\theta) \cos(kz)(I_{v+1}(k\rho) + \frac{v}{k\rho}I_v(k\rho)) \\ +d_{6kv}k \sin(v\theta) \sin(kz)(I_{v+1}(k\rho) + \frac{v}{k\rho}I_v(k\rho)) \\ +d_{7kv}k \cos(v\theta) \sin(kz)(I_{v+1}(k\rho) + \frac{v}{k\rho}I_v(k\rho)) \\ +d_{8kv}k \sin(v\theta) \cos(kz)(I_{v+1}(k\rho) + \frac{v}{k\rho}I_v(k\rho)) \end{array} \right. + \sum_{v=1}^h \left\{ \begin{array}{l} e_{1v}v\rho^{(v-1)} \cos(v\theta) \\ +e_{2v}v\rho^{(v-1)} \sin(v\theta) \\ +e_{3v}vz_i\rho^{(v-1)} \cos(v\theta) \\ +e_{4v}vz_i\rho^{(v-1)} \sin(v\theta) \end{array} \right\}$$

$$\begin{aligned}
& + \bar{a}/\rho + \bar{b}z/\rho \\
& + \sum_{k=1}^g \left\{ \begin{array}{l} -\bar{c}_{1k} k \cosh(kz) Y_1(k\rho) \\ -\bar{c}_{2k} k \sinh(kz) Y_1(k\rho) \\ -\bar{c}_{3k} k \cos(kz) K_1(k\rho) \\ -\bar{c}_{4k} k \sin(kz) K_1(k\rho) \end{array} \right. \\
& + \sum_{v=1}^h \left\{ \begin{array}{l} \bar{d}_{1kv} k \cos(v\theta) \cosh(kz) (-Y_{(v+1)}(k\rho) + \frac{v}{k\rho} Y_v(k\rho)) \\ + \bar{d}_{2kv} k \sin(v\theta) \sinh(kz) (-Y_{(v+1)}(k\rho) + \frac{v}{k\rho} Y_v(k\rho)) \\ + \bar{d}_{3kv} k \cos(v\theta) \sinh(kz) (-Y_{(v+1)}(k\rho) + \frac{v}{k\rho} Y_v(k\rho)) \\ + \bar{d}_{4kv} k \sin(v\theta) \cosh(kz) (-Y_{(v+1)}(k\rho) + \frac{v}{k\rho} Y_v(k\rho)) \\ + \bar{d}_{5kv} k \cos(v\theta) \cos(kz) (-K_{(v+1)}(k\rho) + \frac{v}{k\rho} K_v(k\rho)) \\ + \bar{d}_{6kv} k \sin(v\theta) \sin(kz) (-K_{(v+1)}(k\rho) + \frac{v}{k\rho} K_v(k\rho)) \\ + \bar{d}_{7kv} k \cos(v\theta) \sin(kz) (-K_{(v+1)}(k\rho) + \frac{v}{k\rho} K_v(k\rho)) \\ + \bar{d}_{8kv} k \sin(v\theta) \cos(kz) (-K_{(v+1)}(k\rho) + \frac{v}{k\rho} K_v(k\rho)) \end{array} \right\} \\
& + \sum_{v=1}^h \left\{ \begin{array}{l} -\bar{e}_{1v} v \rho^{-(v-1)} \cos(v\theta) \\ -\bar{e}_{2v} v \rho^{-(v-1)} \sin(v\theta) \\ -\bar{e}_{3v} v z \rho^{-(v-1)} \cos(v\theta) \\ -\bar{e}_{4v} v z \rho^{-(v-1)} \sin(v\theta) \end{array} \right\} \\
U_\theta = & \sum_{k=1}^g \sum_{v=1}^h \left\{ \begin{array}{l} -d_{1kv} v \sin(v\theta) \cosh(kz) J_v(k\rho) \\ + d_{2kv} v \cos(v\theta) \sinh(kz) J_v(k\rho) \\ - d_{3kv} v \sin(v\theta) \sinh(kz) J_v(k\rho) \\ + d_{4kv} v \cos(v\theta) \cosh(kz) J_v(k\rho) \\ - d_{5kv} v \sin(v\theta) \cos(kz) I_v(k\rho) \\ + d_{6kv} v \cos(v\theta) \sin(kz) I_v(k\rho) \\ - d_{7kv} v \sin(v\theta) \sin(kz) I_v(k\rho) \\ + d_{8kv} v \cos(v\theta) \cos(kz) I_v(k\rho) \end{array} \right\} \\
& + \sum_{v=1}^h \left\{ \begin{array}{l} -e_{1v} v \rho^v \sin(v\theta) \\ + e_{2v} v \rho^v \cos(v\theta) \\ - e_{3v} v z \rho^v \sin(v\theta) \\ + e_{4v} v z \rho^v \cos(v\theta) \end{array} \right\} \\
& + \sum_{k=1}^g \sum_{v=1}^h \left\{ \begin{array}{l} -\bar{d}_{1kv} v \sin(v\theta) \cosh(kz) Y_v(k\rho) \\ + \bar{d}_{2kv} v \cos(v\theta) \sinh(kz) Y_v(k\rho) \\ - \bar{d}_{3kv} v \sin(v\theta) \sinh(kz) Y_v(k\rho) \\ + \bar{d}_{4kv} v \cos(v\theta) \cosh(kz) Y_v(k\rho) \\ - \bar{d}_{5kv} v \sin(v\theta) \cos(kz) K_v(k\rho) \\ + \bar{d}_{6kv} v \cos(v\theta) \sin(kz) K_v(k\rho) \\ - \bar{d}_{7kv} v \sin(v\theta) \sin(kz) K_v(k\rho) \\ + \bar{d}_{8kv} v \cos(v\theta) \cos(kz) K_v(k\rho) \end{array} \right\} \\
& + \sum_{v=1}^h \left\{ \begin{array}{l} -\bar{e}_{1v} v \rho^{-v} \sin(v\theta) \\ + \bar{e}_{2v} v \rho^{-v} \cos(v\theta) \\ - \bar{e}_{3v} v z \rho^{-v} \sin(v\theta) \\ + \bar{e}_{4v} v z \rho^{-v} \cos(v\theta) \end{array} \right\}
\end{aligned}$$

$$\begin{aligned}
 U_z = & b + \sum_{k=1}^g \left\{ \begin{aligned} & c_{1k}k \sinh(kz)J_0(k\rho) + c_{2k}k \cosh(kz)J_0(k\rho) \\ & -c_{3k}k \sin(kz)I_0(k\rho) + c_{4k}k \cos(kz)I_0(k\rho) \end{aligned} \right. \\
 & + \sum_{v=1}^h \left\{ \begin{aligned} & d_{1kv}k \cos(v\theta) \sinh(kz)J_v(k\rho) + d_{2kv}k \cos(v\theta) \cosh(kz)J_v(k\rho) \\ & + d_{3kv}k \cos(v\theta) \cosh(kz)J_v(k\rho) + d_{4kv}k \sin(v\theta) \sinh(kz)J_v(k\rho) \\ & - d_{5kv}k \cos(v\theta) \sin(kz)I_v(k\rho) + d_{6kv}k \sin(v\theta) \cos(kz)I_v(k\rho) \\ & + d_{7kv}k \cos(v\theta) \cos(kz)I_v(k\rho) - d_{8kv}k \sin(v\theta) \sin(kz)I_v(k\rho) \end{aligned} \right\} \\
 & + \sum_{v=1}^h \{ e_{3v}\rho^v \cos(v\theta) + e_{4v}\rho^v \sin(v\theta) \} \\
 & + \bar{b} \ln \rho + \sum_{k=1}^g \left\{ \begin{aligned} & \bar{c}_{1k}k \sinh(kz)Y_0(k\rho) + \bar{c}_{2k}k \cosh(kz)Y_0(k\rho) \\ & - \bar{c}_{3k}k \sin(kz)K_0(k\rho) + \bar{c}_{4k}k \cos(kz)K_0(k\rho) \end{aligned} \right. \\
 & + \sum_{v=1}^h \left\{ \begin{aligned} & \bar{d}_{1kv}k \cos(v\theta) \sinh(kz)Y_v(k\rho) + \bar{d}_{2kv}k \sin(v\theta) \cosh(kz)Y_v(k\rho) + \\ & \bar{d}_{3kv}k \cos(v\theta) \cosh(kz)Y_v(k\rho) + \bar{d}_{4kv}k \sin(v\theta) \sinh(kz)Y_v(k\rho) - \\ & \bar{d}_{5kv}k \cos(v\theta) \sin(kz)K_v(k\rho) + \bar{d}_{6kv}k \sin(v\theta) \cos(kz)K_v(k\rho) + \\ & \bar{d}_{7kv}k \cos(v\theta) \cos(kz)K_v(k\rho) - \bar{d}_{8kv}k \sin(v\theta) \sin(kz)K_v(k\rho) \end{aligned} \right\} \\
 & + \sum_{v=1}^h \{ \bar{e}_{3v}\rho^{-v} \cos(v\theta) + \bar{e}_{4v}\rho^{-v} \sin(v\theta) \}
 \end{aligned}$$

$$\frac{\partial \rho}{\partial x} = \cos \theta$$

$$\frac{\partial \theta}{\partial x} = \frac{-\sin \theta}{r}$$

$$\frac{\partial \rho}{\partial y} = \sin \theta$$

$$\frac{\partial \theta}{\partial y} = \frac{\cos \theta}{r}$$

